A0030/79

AGO,1979

CBPF
CENTRO BRASILEIRO
DE PESQUISAS FÍSICAS

PHOTODISINTEGRATION OF LIGHT AND MEDIUM-WEIGHT NUCLEI AT INTERMEDIATE ENERGIES-V MASS-YIELD DEPENDENCE OF TRUE DIRECT (γ,n) AND (γ,p) REACTIONS

J.B. Martins, E.S. de Almeida, V. di Napoli, M.Foshina,
O.A.P. Tavares and M.L.Terranova

RIO DE JANEIRO
BRASIL

PHOTODISINTEGRATION OF LIGHT AND MEDIUM-WEIGHT NUCLEI AT INTERMEDIATE ENERGIES-V

MASS-YIELD DEPENDENCE OF TRUE DIRECT (γ,n) AND (γ,p) REACTIONS

J.B. MARTINS, E.S. DE ALMEIDA[†], V. DI NAPOLI[§], M. FOSHINA and O.A.P. TAVARES

Centro Brasileiro de Pesquisas Físicas-CNPq, Rio de Janeiro, Brasil

and

M.L. TERRANOVA

Istituto di Chimica Generale ed Inorganica dell'Università, Roma, Italia

Abstract-The mass-yield dependence of (γ,n) and (γ,p) reactions in the photon energy range (0.2-1) GeV has been investigated. A Monte Carlo calculation for these reactions has been carried out to compare values of the measured cross sections with those arising from different models of interaction. Very good agreement was found between experiment and estimates based on the simple assumption of a fast-step, direct character of the reaction mechanism. As a result of the analysis, N- and Z-dependences of mean cross sections are given for (γ,n) and (γ,p) reactions, respectively. Agreement with theoretical results based on a more sophisticated formalism is quite reasonable.

[†]Permanent address: Instituto de Física, Universidade Federal Fluminense, Niterói-RJ, Brasil.

[§]On leave of absence from the Istituto di Chimica Generale ed Inorganica dell'Università, Roma, Italia.

INTRODUCTION

Our study of photonuclear reactions at intermediate energies [1-4] has heretofore been concerned mainly with spallation and fragmentation-fission processes occurring in light and medium-weight nuclei.

Processes such as (γ,n) and (γ,p) do contribute, however, to a large extent to the γ-nucleus total interaction cross section. Besides, the study of (γ,n), (γ,p) and (γ,π) reactions can give valuable information about some scarcely known aspects of photon interaction and nuclear structure. All these reactions, in fact, seem to have characteristics quite different from spallation and fission, on one side, and fragmentation, on the other side, and are accredited as predominantly direct.

Above the threshold of π-meson photoproduction, we define as *true direct processes* those originating from the interaction between an incoming photon and a single nucleon inside the target nucleus and leading to the production of a real pion and a recoil nucleon, at least one of which succeeds in escaping, an overall energy being transferred to the rest nucleus well below the minimum amount required to evaporate other particles. Starting from 30-40 MeV up to energies of a few hundred MeV, true direct processes may as well originate from the photodisintegration of small clusters of particles, mostly neutron-proton pairs, if the residual nucleus is left in a truly de-excited state after the escape of some or all these particles.

From this standpoint, only reactions of the type

$$ {}^{A}_{Z}X(\gamma,n)^{A-1}_{Z}X \qquad (1) $$

$$ {}^{A}_{Z}X(\gamma,p)^{A-1}_{Z-1}Y \qquad (2) $$

$$ {}^{A}_{Z}X(\gamma,\pi^{0})^{A}_{Z}X \qquad (3) $$

$$ {}^{A}_{Z}X(\gamma,\pi^{+})_{Z-1}{}^{A}Y \qquad (4) $$

$$ {}^{A}_{Z}X(\gamma,\pi^{-})_{Z+1}{}^{A}Y \qquad (5) $$

$$ {}^{A}_{Z}X(\gamma,np)^{A-2}_{Z-1}Y \quad , \qquad (6) $$

where ${}^{A}_{Z}X$ denotes a target nucleus of atomic number Z and mass number A, must be considered, to which the following primary interactions will contribute

$$ \gamma + n \rightarrow n + \pi^{0} \qquad (7) $$

$$ \gamma + n \rightarrow p + \pi^{-} \qquad (8) $$

$$ \gamma + p \rightarrow p + \pi^{0} \qquad (9) $$

$$ \gamma + p \rightarrow n + \pi^{+} \qquad (10) $$

$$ \gamma + (np) \rightarrow n + p^{\S} \qquad (11) $$

in this very peculiar sense that reaction (1) originates from (7) and (8), (2) from (9) and (10), (3-5) from (7-10), and (6) from (11). We wish further to point out that any contribution to reactions (1) and (2) from the interaction between the incident photon and a neutron-proton pair (e.g. through the so-called "quasi-deuteron" mechanism of interaction) cannot be taken into account due to kinematical restrictions [6].

---

§ A more recent and rigorous model [5] treats this interaction in terms of exchange of a virtual meson between correlated neutron-proton pairs. We shall not discuss, however, interaction (11) thoroughly, since from both models contributions either negligible or null at all are deduced for the reactions which we are dealt with (see also Ref. [6]).

Up to the present time, a few papers have been published aiming to interpret the mass-yield distribution of reactions (1-5) in complex nuclei at intermediate energies [7-12], and we believe that a careful analysis of the experimental cross section data for these reactions and an estimate of their yields by means of a Monte Carlo calculation may result in a better understanding of the intermediate- and high-energy γ-nucleus interaction.

As far as (γ,n) and (γ,p) reactions are concerned, the interaction model proposed in Refs. [7,8] was essentially developed for light nuclei, and a very heavy contribution from the quasi-deuteron mechanism was assumed as being effective, still at energies above about 100 MeV. On the other hand, analyses made in Refs. [9,10] suffered some limitations, either being only of a semiempirical character [9] or affected by simplifications and approximations introduced in order to make easier the calculation of the cascade step [10]; moreover, both were merely devoted to (γ,n) reaction. Also, in the case of (γ,xn) $(x > 1)$ reactions [13], the treatment did not distinguish between the *non-direct* part of the interaction and a possible *quasi-direct* contribution (i.e. cascade events not "contaminated" from evaporation contribution).

Experimental data on (γ,n)[†] and (γ,p) [8,14-20] reactions in complex nuclei at energies from the pion photoproduction threshold up to 1 GeV are relatively poor, those for (γ,n) being approximately three times more numerous and, what is even more important, physically more reliable[§] than for (γ,p) reaction.

[†] A complete list of references regarding (γ,n) cross section measurements is given in Refs. [9,10], which the reader is referred to.

[§] This is perhaps due to difficulties in the measurements of some (γ,p) cross sections.

The present paper will be dealt with the study of the *true direct* contribution to the yields of (γ,n) and (γ,p) processes. For the sake of completeness, target nuclei will be considered up to the heavy mass region ($7 \leq A \leq 238$). A future paper will be entirely devoted to a deeper discussion about γ-pion reactions.

ANALYSIS OF THE MEASURED (γ,p) YIELDS

The yield of a photonuclear reaction for a given target as a function of the incident energy is often very difficult to measure. The absence of monochromatic photon sources in the energy range under consideration makes bremsstrahlung the unique tool capable of giving photon beams of sufficiently high intensity. Unfortunately, a bremsstrahlung beam is constituted by photons with energies k ranging from zero up to the so-called bremsstrahlung end-point energy, E_o, with an approximate energy distribution of the type $1/k$. This implies a toilsome transformation [21] from bremsstrahlung yields (in general expressed as cross sections per equivalent quantum, σ_Q) to photon yields (absolute cross sections or cross sections per photon, σ_k). Very frequently, the trend of the σ_Q values vs the energy E_o does not permit to obtain any structure for σ_k and then it turns out more preferable to calculate the mean cross section $\overline{\sigma}_k$ within the E_o range explored. In this situation, the approximation of the square shape of the bremsstrahlung spectra can suffice. Sometimes the measured σ_Q values appear so spread, when plotted against E_o, that no more than quite rough estimates of the order or magnitude of $\overline{\sigma}_k$ may be achieved.

Cross section measurements of (γ,p) reactions have been reported for the following nuclei: ^{11}B [16], ^{16}O [15], ^{18}O [14], ^{30}Si [8,19], ^{40}Ca [18], ^{68}Zn [19], ^{118}Sn [17,20], and ^{130}Te [19]. For ^{30}Si, ^{68}Zn, ^{118}Sn, and ^{130}Te the induced radioactivity method was employed to determine the cross sections per equivalent quantum. For the others, different physical methods were necessary.

When examining the experimental data, we arrived at the conclusion that for but six target nuclei the σ_Q measurements furnished values suitable to be fitted as to give mean cross sections per photon: ^{11}B, ^{18}O, ^{30}Si, ^{68}Zn, ^{118}Sn, and ^{130}Te. Furthermore, the spreading of σ_Q's vs E_o and the error affecting each measurement were so large that we preferred, for each reaction, to fit two straight lines through the experimental points, the first having the maximum slope and the second the minimum slope, thus obtaining "ranges of uncertainty of" instead of "single valued" mean cross sections per photon. It should be noted, at this point, that our fits for (γ,p) reactions did not take into consideration any subtraction of tails arising from interactions typical of lower energy regions (see Introduction). For the sake of comparison (see next section), the cross sections were averaged over the energy range 0.2 GeV-1 GeV. The averaging procedure was made in the following manner: if the measures arrived at E_o = 0.8 GeV, it was assumed that the same trend of σ_Q vs E_o was valid up to 1 GeV; in the case of $^{18}O(\gamma,p)^{17}N$ reaction the measures stopped at about 0.4 GeV, and we assumed that above 0.4 GeV the trend of σ_k vs k was the same we calculated (see next section), thus we used a normalization factor to calculate $\bar{\sigma}_k$ in the energy region 0.2GeV-1GeV.

Once obtained these cross sections, we plotted them in a log-log graph against the atomic number Z of the target nucleus, as one can see in Fig. 1. A least-squares analysis gave the following dependence of $\bar{\sigma}_k$ on Z: $\bar{\sigma}_k = (115 \pm 15)Z^{(0.50\pm0.05)}$, $\bar{\sigma}_k$ being expressed in μb. From the fit, the point relative to ^{30}Si was rejected. Table 1 reports the mean cross sections $\bar{\sigma}_k$ obtained as described above for (γ,p) reactions.

THE MONTE CARLO CALCULATION

The essentials of the Monte Carlo calculation have already been described in [10]. We shall indicate here some important modifications we made in order to improve the calculation itself and, at the same time, to account for more severe physical restrictions.

The target nucleus is described in terms of degenerate Fermi gases of Z protons and N neutrons confined within a spherically symmetric nuclear potential of radius $R = r_0 A^{1/3}$. Different values of r_0 were assumed according to the A-dependence of the form $r_0 = 1.12 + 2.35A^{-2/3} - 2.07A^{-4/3}$, where r_0 is expressed in fm [22].

Different cutoff energies were chosen for neutron and proton, as functions of the nuclear parameters which characterize the target nucleus, thus introducing in the calculation some information on the nuclear structure.

To be sure that the residual nucleus be truly "cold" after the cascade step (i.e. no evaporation occured at all), a

residual excitation energy of 2 MeV has been imposed as an upper limit. This perhaps is the most important change with respect to the old calculation [10] . The choice of 2 MeV was not a casual one, but this point will be discussed later.

In the development of cascades, the Pauli exclusion principle was always accounted for whenever the allowance of a particle-particle collision had to be verified.

The mechanisms of primary interaction of the photon were considered to be the photomesonic and the quasi-deuteron ones. The points of interaction of the incoming photons have been assumed as uniformly distributed within the nucleus, so treating *a priori* this interaction within the framework of a "nuclear volume" model [23]. In the case of the quasi-deuteron interaction the dependence of the Levinger's factor L on the mass number A has been taken as $L = 2.1\, \ell n\, (1.3A)$, since it gives values of L which agree quite well with those experimentally determined. Due to the smallness of the deuteron photodisintegration cross section we cut off the contribution of quasi-deuteron interaction at 0.6 GeV.

We considered all the possible interactions of the incoming photon via the photomesonic model. As the photoproduction of more than a single pion implies a very large energy transfer to the nucleus, we based the calculation simply on one-pion production, but, above 0.4 GeV, the number of cascade events was normalized by multiplying it by the ratio $(\sigma_o - \sigma_{\pi>1})/\sigma_o$, where σ_o is the total inelastic photon-nucleon (proton) cross section and $\sigma_{\pi>1}$ the sum of the cross sections of all those contributions (e.g. baryon resonances) leading to the creation of more than one pion.

A total number of 10^4 to 4×10^4 cascades (according to the likelihood of the process under study) was followed for each energy of the incident photon. The probability $\phi_i(A,k)$ that a particular reaction i occurred during the cascade step was then calculated as the ratio of the effective number of cascades which led to reaction i to the total number of cascades. Consequently, its cross section is given by

$$\sigma_{k,i} = \phi_i(A,k)\left[A\sigma_o(k) + L\,\frac{NZ}{A}\,\sigma_D(k)\right] \quad , \qquad (12)$$

where σ_D is the cross section of deuteron photodisintegration (data on σ_o and σ_D have been taken from [24] and [25], respectively).

RESULTS OF THE CALCULATION

A total of 23 nuclei, from ^{7}Li up to ^{238}U, and 20 different photon energies, from 0.15 GeV up to 1 GeV, have been considered in the course of the calculation. For some representative nuclei and for a reduced number of photon energies, different maximum excitation energies E^* of the residual post-cascade nucleus have also been tested (from 2 MeV up to 40 MeV), in order to examine the influence of this parameter on the calculated cross sections.

We outline here the most interesting results obtained for (γ,n) and (γ,p) reactions:

i) as we might expect, no contribution from the quasi-deuteron mechanism of interaction (neither direct nor even from cascade)

was found irrespective of the E^* values chosen. It can be concluded that, above 0.15 GeV, (γ,n) and (γ,p) events originate from photomesonic effects.

ii) (γ,n) events arise from the following primary interactions: $\gamma+n \rightarrow n+\pi^0$ and $\gamma+n \rightarrow p+\pi^-$, only a few cases deriving from γ-proton photomesonic primary interaction and hence from a fast cascade process. For ^{27}Al and for $E^* \leq 2$ MeV, the contribution of both interactions (7) and (8) represents 90% of the total at k = 0.2GeV, and about 100% at k = 1 GeV. The same trend is encountered for (γ,p) reactions, for which interactions (9) and (10) play the role of (7) and (8).

iii) (γ,n) direct events arising from (7) and (8) are parted as follows: approximately 40% from (7) and 60% from (8), more or less independently from k,A,E^*. For (γ,p), similarly, 45% from (9) and 55% from (10), still without any significant dependence on k,A,E^*.

iv) the general trend of $\phi(A,k)$ as a function of k shows two bumps centred at about 0.3 GeV (the region of the Δ-1236 resonance) and 0.7 GeV, this latter quite large in width. For light nuclei (say, up to A = 30) ϕ decreases slowly with increasing k for $k > 0.3$GeV, while it remains nearly constant for medium-weight and heavy nuclei and increases with k for ^{238}U. A sharp increase of ϕ with increasing k is always found from 0.2 GeV up to 0.3 GeV. Also, the trend of ϕ turns out to be more flattened for (γ,p) than for (γ,n) direct processes.

v) the mean values of σ_k in the energy range 0.2-1 GeV of (γ,n) reactions are higher than the corresponding values of (γ,p) reactions. The ratio $\bar{\sigma}_{k(\gamma,n)}/\bar{\sigma}_{k(\gamma,p)}$, even being constantly higher than,

is however very close to the nuclear parameter N/Z, which suggests that the influence of cutoff energies, though different for proton and neutron, is almost completely levelled off by the mechanisms of primary interactions (this point will be discussed further).

vi) the total number of (γ,n) and (γ,p) reactions leading to a residual nucleus, either "cold" or "hot", is clearly constant (for a given target nucleus and incident energy). What varies with the excitation energy is the ratio of "cold" to "hot plus cold" (total) events. Whatever E^*, this ratio is very small up to k = 0.2 GeV, but becomes larger as the photon energy increases, and this is also due to the fact that "hot events" from the quasi-deuteron interaction become smaller.

Tables 2 and 3 report values of ϕ for 15 representative nuclei at 17 incident photon energies. In Figs. 2 and 3 the mean cross sections per photon are plotted as a function of the mass number of the target nucleus. In these figures, $\overline{\sigma}_k$ values have been reported which were obtained with the following assumptions: subtraction of two-pion photoproduction (upper values), henceforth abridged as Appr. I; subtraction of two-pion plus three-pion contributions (medium values), Appr. II, following Refs. [26,27], and subtraction of the contribution of all interaction and baryon resonances decaying into more than one meson (lower values), Appr. III. The trend of $\overline{\sigma}_k$ (Appr. I) of (γ,n) vs A of Ref. [10] ($A^{0.86}$) has been reported for the sake of comparison. The errors indicated in the figures or in the formulae are statistical only.

In the next section we shall discuss in detail all these results.

DISCUSSION AND CONCLUSIONS

A least-squares analysis made with the Monte Carlo results gave the A-dependence for the mean cross sections of (γ,n) and (γ,p) reactions, in the energy range 0.2 GeV - 1 GeV, of the general type

$$\bar{\sigma}_{k(\gamma,N)} = aA^b \qquad (13)$$

(N stands for 1-nucleon, neutron or proton), with the following values of the parameters a and b

$$\begin{aligned} a &= (78 \pm 7)\mu b \ , \ b = 0.67 \pm 0.01 \quad \text{(Appr. I)} \\ a &= (75 \pm 7)\mu b \ , \ b = 0.67 \pm 0.01 \quad \text{(Appr. II)} \\ a &= (67 \pm 6)\mu b \ , \ b = 0.66 \pm 0.01 \quad \text{(Appr. III)} \end{aligned} \qquad (13a)$$

for (γ,n) reactions, and

$$\begin{aligned} a &= (93 \pm 9)\mu b \ , \ b = 0.565 \pm 0.008 \quad \text{(Appr. I)} \\ a &= (95 \pm 9)\mu b \ , \ b = 0.560 \pm 0.008 \quad \text{(Appr. II)} \\ a &= (81 \pm 8)\mu b \ , \ b = 0.544 \pm 0.008 \quad \text{(Appr.III)} \end{aligned} \qquad (13b)$$

for (γ,p) reactions.

In the graphs of Figs. 2 and 3 only the least-squares straight lines relative to Appr. III have been drawn to make figures more clear. If one compares eqn (13a) (Appr. I) with the equation

$$\bar{\sigma}_{k(\gamma,n)} = (63 \pm 6)A^{(0.860\pm0.012)} \qquad (14)$$

given in [10] , two interesting considerations has to make. First, the two coefficients (78±7)μb and (63±6)μb (eqn (14)) are practically alike, if the statistical uncertainties are properly taken

into account, thus indicating that the primary interactions which dominate the entire process still remain the same (see also Ref. [10]). Second, a remarkable difference is found between the exponents (0.67 ± 0.01) and (0.860 ± 0.012) (eqn (14), Ref. [10]). From both a numerical and a physical point of view, the difference is not so astonishing. More restrictive physical input information would clearly lead to an A-dependence less than 0.86. On the other hand, the ratio F of the mean cross sections from eqn (14) to the mean cross sections from eqn (13a), Appr. I, is

$$F = 0.8A^{0.19} \quad , \qquad (15)$$

that is, mean cross sections of (γ,n) reactions are reproduced with a satisfactorily good agreement by both eqns (13a) and (14) in the mass region up to 20. The agreement becomes less satisfactory as A increases, but the ratio F never exceeds 1.9, this latter value being reached at A = 238. A still better agreement is achieved with $\bar{\sigma}_{k(\gamma,n)} = 0.104A^{0.81}$ μb as given in [9].

Values of the exponents in eqn (13), which are as an average 0.67 for (γ,n) reaction and 0.56 for (γ,p) reaction, need however for a deeper discussion. An $A^{0.67}$-dependence of $\bar{\sigma}_{k(\gamma,n)}$ would seem to suggest a "surface model" of interaction [23] which predicts an $A^{2/3}$-dependence. But one must remember that the calculation was carried out with the very explicit assumption of a "volume" (A^1) interaction. The fact then that the dependences found for (γ,n) and (γ,p) reactions at intermediate energies turn out as $A^{\sim 0.67}$ and $A^{\sim 0.56}$, respectively,

should be ascribed to a strong π-meson reabsorption and/or nucleon-nucleon interaction in the bulk of the nucleus (strong "hindrance factor"), as well as to cutoff parameters†. These conclusions were already suggested in [23] and experimentally proved, although for π^--photoproduction at energies somewhat higher, as reported in [28]. We can go a little further. The hindrance factor for (γ,N) reactions is greatly influenced by the cutoff parameters (cutoff energies and upper limit of excitation energies). We anticipate here that for π-meson photoproduction, where no cutoff energies have been considered and the excitation energy was the sole cutoff parameter, an $A^{>0.8}$-dependence is found for the cross sections relative to these processes.

Some words must be spent here about the upper limit of 2 MeV taken as the excitation energy E^* which guarantees that particle evaporation does not occur for the post-cascade nucleus. Although this parameter revealed itself as not extremely important (for 2 MeV $\leq E^* <$ 40 MeV) for (γ,n) and (γ,p) reactions, while playing a fundamental role in (γ,π) reactions, it shows however some weight, for the number of events favourable slightly decreases

---

† It would be very tedious and time consuming to discuss here in full detail how suppression of cold (γ,n) and (γ,p) events is governed by particle reabsorption and cutoff energies. We shall confine ourselves to a brief description of some effects which seem apparently in conflict with each other. If we assume the (γ,n) reaction as an example, we note (see previous section) that, being the primary interaction (8) a factor ≃ 1.5 more effective than (7), the Coulomb barrier will influence (γ,n) to an extent which ought to be more large than for (γ,p), so far as nucleon escaping is concerned. On the other hand, the ratio N/Z for medium-weight and heavy nuclei obviously makes (γ,n) more likely than (γ,p). Finally, for the primary interactions (7) and (9), one must consider that π^0-mesons can be reabsorbed by nn, pp and np pairs, while for (8) and (10), π^-- and π^+-mesons only by np and pp or np and nn pairs, respectively. All these facts, taken together, cause $\phi_{(\gamma,n)}$ to be in general higher than $\phi_{(\gamma,p)}$ (at least at the lower energies) and both to decrease with increasing A.

with E^*. To evaporate a neutron, a minimum amount of energy of about 7 MeV is necessary. So, excitation energies in excess of 7 MeV cannot be taken into consideration. In Fig. 4, also in this case anticipating results that will be published in a complete form in a further paper, we report some eye-fitted curves which represent, at each E^*, the percentage of the "cold" yields of (γ,π) events (sum of π^0, π^+ and π^-) with respect to the sum of "cold plus hot" yields, as a function of the photon incident energy, in the case of a ^{27}Al target nucleus. The curves marked 40 and 10 (i.e. E^* = 40 MeV and E^* = 10 MeV) are evidently without any significance. They were reported for the mere scope of comparison. The curves marked 5 and 3 are also somewhat irreal, for it is very hard to accept so high yields of cold (γ,π) reactions at energies between 0.15 and 0.20 GeV, while the experimental data for such reactions furnish yields of the order of a few microbarns. Consequently, we were forced to keep $E^* \leq 2$ MeV, as the curve which best fitted the experimental response.

Other important results of the calculations regard, as said, the numbers of (γ,n) events arising from neutron target and (γ,p) from proton target. These events represent almost the total (γ,n) and (γ,p) events. This is a reason more to consider the (γ,N) processes as essentially direct. Taking into consideration the σ_k values obtained with Appr. III, and by subtracting the non-direct part, we obtain the cross section of those processes we defined as *true direct*. With this in mind, we thought more convenient to search for a relation between $\overline{\sigma}_{k(\gamma,n)}$ and N, and $\overline{\sigma}_{k(\gamma,p)}$ and Z. The straight lines of Figs. 5 and 6 are least-squares fits giving the N- and Z-dependences of $\overline{\sigma}_{k(\gamma,n)}$ and $\overline{\sigma}_{k(\gamma,p)}$ respectively, whose equations are

$$\bar{\sigma}_{k(\gamma,n)\text{true direct}} = (120 \pm 11)N^{(0.60\pm0.01)}\ \mu b \qquad (16)$$

$$\bar{\sigma}_{k(\gamma,p)\text{true direct}} = (124 \pm 12)Z^{(0.53\pm0.01)}\ \mu b \quad . \qquad (17)$$

In all fits (eqns (13), (16) and (17)) the points relative to the lighter nuclei (Li, Be, B, and perhaps C) lie always off the least-squares lines. This may be explained in a very simple manner. We considered the nucleus essentially as a degenerate Fermi gas of protons and neutrons, but such an assumption may fail for ensembles of 3 to 6 nucleons. Also, for these nuclei the cutoff energies can exert an exaggerated weight. As a matter of fact, though, the deviations are quite small, and eqns (16) and (17) must be considered valid for the whole mass range studied. Other small deviations from the straight lines may be imputed in part to some shell effects which have indirectly been accounted for in the choice of the cutoff energies (e.g. ^{12}C, ^{16}O-^{18}O, ^{40}Ca, ^{118}Sn-^{130}Te)

The levelling off suffered by the cutoff energies (due to different contributions of interactions (7-10)) (see Introduction) becomes quite clear when searching to unfold the numerical values of the exponents in eqns (16,17) in terms of these cutoff energies, taking in due account the weight of each primary interaction. With a sufficient degree of approximation, the unfolding procedure was made with the simple assumption that the mass number A-1 of the residual nucleus be the unique independent variable. We succeeded hence in obtaining

$$\sigma_{(\gamma,n)\text{true direct}}(A,N) = 120N\exp\left[-0.36(A-1)^{0.32}\right]\mu b \qquad (18)$$

and

$$\sigma_{(\gamma,p)\text{true direct}}(A,Z) = 124Z\exp\left[-0.44(A-1)^{0.29}\right]\mu b \qquad (19)$$

for (γ,n) and (γ,p) reactions, respectively. These two equations reproduce the results of (16) and (17) within ± 15% (10% for the (γ,n) reaction) and this is further proved by the fact that, within ± 15%, the two factors $120\exp\left[-0.36(A-1)^{0.32}\right]$ and $124\exp\left[-0.44(A-1)^{0.29}\right]$ give approximately the same values, only being A-dependent, as one can immediately see in Table 4, where the ratio $Q = (120\exp\left[-0.36(A-1)^{0.32}\right])/(120\exp\left[-0.44(A-1)^{0.29}\right])$ is reported for six target masses covering the whole region investigated.

Some stress would we like to put on the following. Given a target with mass number A, Q represents the ratio of the mean (γ,n) cross section per neutron to the mean (γ,p) cross section per proton, as obtained from (18) and (19). The fact then that its values are practically constant and equal to unity, further supports the idea of a strong dependence of the yields of true direct reactions on the number of proper target nucleons (we wish advertise that errors which affect Q are somewhat large; figures after the first decimal are, in any case, without physical significance and were written in the Table for the sole purpose of making clearer what we attempted to say).

The numerical value of the exponents in eqns (16) and (17) are very near to those of eqns (13), and hence a similar interpretation for these dependences may be invoked.

As regards the coefficients 120 μb and 124 μb, it is readily seen that they are nearly equal to the weighted mean of the cross sections of the elementary interactions $\gamma+n \to n+\pi^0$ and $\gamma+n \to p+\pi^-$ (for (γ,n) reactions), and $\gamma+p \to p+\pi^0$ and $\gamma+p \to n+\pi^+$ (for (γ,p) reactions), whose value is about 90 μb (average value in the energy range 0.2 GeV-1 GeV). This may be

assumed as a further evidence for the photomesonic nature of the reactions under study.

An additional proof of the correctness of the calculation and, consequently, of our hypothesis regarding the mainly direct character of (γ,N) reactions, can be achieved from the trend of the (γ,np) reaction. If one assumes the quasi-deuteron mechanism of interaction be valid at energies above 0.15 GeV, the greatest part of the reaction (6) should arise from the primary interaction (11), while the others should contribute to a much less extent. Moreover, it can be easily inferred that, whatever the E^* value used as cut, the ratio between "cold" and "hot" (γ,np) events from (11) should remain nearly constant. Some tests have been made on a few number of nuclei at different energies and the results confirmed, without any doubt, the assumptions made. Table 5 summarizes the results obtained for ^{27}Al at 0.3 GeV. In this Table the number of events relative to the (γ,n) and (γ,p) reactions are reported for comparison.

After a discussion, as complete as possible and perhaps tedious to some extent, of the results of our calculation, we can start soon with a comparison between calculated and measured cross sections for (γ,n) and (γ,p) reactions, also comparing both these with the theoretical predictions mainly based on the very interesting treatment given by Andersson *et al.* [7], which up now still remains as the more complete and useful theory about photomesonic direct processes.

In Fig. 7, the trend is reported of $\sigma_{k(\gamma,n)}$ for ^{12}C as a function of k. An overall good agreement is obtained for the three curves drawn in the graph. They represent the measured trend [29] (full line), obtained trend from the present calcul-

ation (Appr. III, dash-dotted line), and the resulting trend from [7] (dashed line). The calculated curves and the experimental one do agree with each other in a satisfactory manner. The largest discrepancy is met at about 0.3 GeV (a factor $\lesssim 2$) and in the immediate vicinity of this resonance-like peak (from the Δ-1236 baryon resonance). Discrepancies tend to disappear by increasing energy k . An agreement quite good is also found between both calculated curves. For other (γ,n) reactions, the reader is kindly referred to [9,10] to make a comparison, but taking this in his mind that experimental data there reported are, almost completely, mean cross sections per photon.

In Figs. 8, 9, 10 and 11 we report data on (γ,p) reactions. In Fig. 8 the calculated trend (present work) is shown of σ_k as a function of k for $^{30}Si(\gamma,p)^{29}Al$ reaction (full line). The dashed straight line represents the mean value of these σ_k over the (0.2-1) GeV range. Also reported in the figure are the measured mean value from [19] (dash-dotted line) and four points calculated accordingly to the formalism reported in [7,8] . In this case also, results from both calculations seem to agree quite well, while the same is clearly not true for the experimental $\bar{\sigma}_k$ reported. Another calculated $\bar{\sigma}_k$ value for the same reaction [8] has not been reported in the graph, since it is some 15% higher than that of [19] , in the same energy range, and the experimental σ_Q measurements are given not above about 0.6 GeV.

Shown in Fig. 9 is a situation quite opposite to that illustrated in the previous figure. It easily seen, in fact, that for $^{68}Zn(\gamma,p)^{67}Cu$, the full line representing the trend of σ_k (present work) and the mean cross section (dashed straight line)

agree well with the measured $\bar{\sigma}_k$ value [19] (dash-dotted line). Though, for this reaction, calculated points following [7,8] show a rather bad agreement with the results of the present calculation and with experimental results. Difficulties will arise when attempting to explain such discrepancies.

The trends of σ_k for $^{118}Sn(\gamma,p)^{117}In^{g+m}$ are given in Fig. 10, where a number of data, either from calculations or experiment, are reported as well. The full curve up to 1 GeV is the result of the present calculation. Full curve up to 0.5 GeV has been experimentally deduced [17]. The open circles represent points calculated following [7,8], as reported in [17]. Plotted in the figure also are found some points (marked with x), which were calculated still following [7,8], but with some heavy change of the physical parameters, aiming to fit better the experimental curve [20]. Points marked with crosses have been calculated in [17] by using a Monte Carlo calculation based on very different physical assumptions [30]. The best agreement is found between the points (o) [17] and the curve of the present calculation, but reasonable agreement is as well found with the experimental curve.

Finally, Fig. 11 shows data for $^{130}Te(\gamma,p)^{129}Sb$. The full line is the result of the present calculation. The mean cross section obtained from the curve is represented by a dashed line. The shadowed strip stands for the range of uncertainty of the experimental mean cross section [19]. Points are calculated [19] following the theoretical interaction model of [7,8]. Good agreement is indeed found between the present calculation and the points obtained by the other theory.

We must advertise that the present calculated values or trends, reported in these figures, are relative to Appr. III for true direct reactions. For experimental trends and related problems, the reader is referred to Table 1.

Before we can conclude this paper, we shall even discuss, at this crucial point, about a number of very interesting interpretations of (γ,N) mechanisms, that, at least in part, have already been mentioned above, for the sake of arriving to keep clear some questions still open.

The theoretical model proposed by Andersson *et al.* [7,8], which for many years has been the basis for calculations of (γ,n) and (γ,p) yields, account for a somewhat larger number of physical quantities we owe to illustrate briefly. In the treatment, they consider a nuclear potential of the Woods-Saxon type

$$V = \frac{V_o}{1 + \exp\left[(r-c)/a\right]} ,$$

where V_o is the sum of Fermi energy at the botton of the potential well plus the appropriate separation (not "binding") energy for nucleons. A potential of the type used in [7,8] contains two parameters ($c = r_o A^{1/3}$ and a) which have often been varied with a certain degree of arbitrariness in the course of further calculations to fit experimental data (see, for example, the data reported in Fig. 10). The kinetic energy of the target nucleon has been introduced in the kinematics, but it was chosen as a constant (30 MeV for light nuclei), what appears rather a crude approximation . Such a value becomes so the crucial parameter in the calculation at lower energies, since a 30-MeV nucleon has a momentum of 239 MeV/c,

that is, a value higher than that of the inpinging photon up to k = 239 MeV. Our calculation, on the contrary, assumes a zero kinetic energy for the target nucleon, as the most probable energy arising from a gaussian-shaped momentum distribution. This is too a rather crude estimate, but we must consider that our analysis was not aimed to arrive at higher degrees of refinements.

According to Andersson *et al.* [7,8] , the nucleus is divided into three different zones with constant potentials (and, consequently, densities), and the probability densities of target nucleons are derived from an harmonic oscillator potential, only a few nucleons in outer shells being thus available as true targets (e.g. 4 protons in the 1p shell for ^{12}C). Other assumptions more or less arbitrary, which can however affect heavily the calculation, concern pion and isobar (e.g. Δ-1236) potentials, assumed in the course of the analysis, to be the same as the nuclear potential.

Apart from these many and remarkable differences, a few but important assumptions are, however, the same either in [7,8] or in the present calculation. To get an idea, the same hypothesis of an interaction between the photon and single nucleon that does not initially affect the residual A-1 system is at the origin of the calculations. This is of the greatest importance for the kinematics of the very primary interactions, mostly at the lower energies (where the Pauli exclusion principle would forbid any interaction, where it not for interactions via baryon resonances). Both calculations have been based on photomesonic models and, furthermore, use has been made of relativistic kinematics [31] and classical trajectories [32] inside the nucleus.

So far as the Monte Carlo calculations on bremsstrahlung-

-induced reactions of Gabriel and Alsmiller [30] are concerned, three distinct zones, each having constant nucleon density, have been considered in this case too. Such a refinement, as we already said, is quite often in striking contradiction with the uncertainties (statistical plus measurements) and scarceness of experimental data. As a matter of fact, then, these calculations do not seem to reproduce (γ,n) and (γ,p) yields with sufficient reliability and extend up to about 0.4 GeV. For further details, the reader is referred to the original paper [30].

In conclusion we wish to underline the most prominent features resulting from the present work analysis of (γ,n) and (γ,p) reactions. These have shown characteristics of essentially true direct interactions and seem clearly governed, in our very simple model, by the kinematics of the initial γ-nucleon interaction, the N/Z ratio of the target nucleus, and by the so-called cutoff parameters (cutoff energies and E^*). The true direct character of the reactions under study seem to be more manifested for (γ,p), where the agreement between experimental and calculated trends has to be considered excellent, in spite of the poorness of the formers. For (γ,n), some discrepancy is met with experiment, mainly in the heavier region of masses [9].

That this would mean a contribution far from negligible from collective effects, it is still an open question. Surely energy considerations would make such a contribution larger for (γ,n) than for (γ,p) reactions (Coulomb barrier should have its proper influence in this evenience). Very peculiar kinematical conditions may well allow a recoil nucleon to enter a bound state and a π-meson to escape the nucleus or even be absorbed in it. Our very hypothetical considerations are looking in particular at

the π^0-meson photoproduction. Nuclear evaporation of a single neutron in competition with γ-emission may then occur in the slow step, and if one looks, once still, at the primary interactions (7) and (9), one has to conclude that, with respect to 1-proton evaporation, 1-neutron evaporation should dominate this particular process. All this, however, is very hard, even to calculate.

Acknowledgements-Some participation of A.M.A. Chamis in the very early stage of the calculations is gratefully acknowledged. We wish to express our deeper thanks to Prof. H.G. de Carvalho and Prof. F. Salvetti for their utmost useful criticism, suggestions and encouragement. The tireless assistance of Mr. A.J.L. Botelho and other members of the computer staff of the CBPF is also gratefully acknowledged. V. di Napoli would like to thank the Centro Brasileiro de Pesquisas Físicas for the extremely warm hospitality he received during the development of the present work. Finally, the authors wish to express their indebtedness with Mrs. H.S. Ferreira for her careful work, never limited to mere brilliantly typewriting the manuscript.

REFERENCES

1. V. di Napoli, G. Rosa, F. Salvetti, M.L. Terranova, H. G. de Carvalho, J.B. Martins and O.A.P. Tavares, *J. inorg. nucl. Chem.* 37, 1101 (1975).

2. V. di Napoli, G. Rosa, F. Salvetti, M.L. Terranova , H. G. de Carvalho, J.B. Martins and O.A.P. Tavares , *J. inorg. nucl. Chem.* 38, 1 (1976).

3. V. di Napoli, F. Salvetti, M.L. Terranova, H.G. de Carva - lho, J.B. Martins and O.A.P. Tavares, *J. inorg. nucl.Chem.* 40, 175 (1978).

4. V. di Napoli, J.B. Martins, G. Rosa, F. Salvetti, O.A.P. Tavares, M.L. Terranova and H.G. de Carvalho, *J. inorg. nucl. Chem.* 40, 1619 (1978).

5. H. Hebach, A. Wortberg and M. Gari, *Nucl. Phys.* A267 , 425 (1976).

6. V. di Napoli, M.L. Terranova, J.B. Martins, J.D. Pinheiro Filho and O.A.P. Tavares, *Lett. Nuovo Cimento* 23,424(1978).

7. G. Andersson, B. Forkman and B. Friberg, *Nucl. Phys.* A171, 529 (1971).

8. B. Friberg, G. Andersson and B. Forkman, *Nucl. Phys.*A171, 551 (1971).

9. V. di Napoli, F. Salvetti, M.L. Terranova, H.G. de Carva - lho, J.B. Martins and O.A.P. Tavares, *Gazz. Chim. Ital.* 105, 317 (1975).

10. H.G. de Carvalho, M. Foshina, J.D. Pinheiro Filho, V. di Napoli, J.B. Martins, F. Salvetti, O.A.P. Tavares and M.L. Terraneva, *Rev. Bras. Fis.* 8, 51 (1978).

11. G. Nydahl and B. Forkman, *Nucl. Phys.* B7, 97 (1968); I. Blomqvist, G. Nydahl and B. Forkman, *Nucl.Phys.* A162 , 193 (1971).

12. I. Blomqvist, P. Janeček, G.G. Jonsson, H. Dinter, K.Tesch, N. Freed and P.Ostrander, *Phys. Rev.* C15, 988 (1977).

13. V. di Napoli, M.L. Terranova, H.G. de Carvalho, J.B. Martins, J.D. Pinheiro Filho and O.A.P. Tavares, *J. inorg. nucl. Chem.* 39, 1727 (1977).

14. D. Reagan, *Phys. Rev.* 100, 113 (1955).

15. J.-O. Adler, G. Andersson, B. Forkman, G.G. Jonsson and K. Lindgren, *Nucl. Phys.* A171, 560 (1971).

16. J.-O. Adler, G.G. Jonsson and K. Lindgren, *Nucl.Phys.*A239, 440 (1975).

17. B. Bülow, M. Eriksson and G.G. Jonsson, *Z. Physik* A275,261 (1975).

18. J.-O. Adler, B. Bülow, G.G. Jonsson and K. Lindgren , *Nucl. Phys.* A280, 325 (1977).

19. B. Bülow, B. Jonsson and M. Nilsson, *Z. Physik* A282 , 261 (1977).

20. G. Andersson, B. Bülow, B. Johnsson, G.G. Jonsson and M. Nilsson, *Z. Physik* A285, 335 (1978).

21. K. Tesch, *Nucl. Instr. Methods* 95, 245 (1971).

22. L.R.B. Elton, *Introductory Nuclear Theory*, Pitman, London (1965).

23. V. di Napoli, *Lett. Nuovo Cimento* 12, 609 (1975).

24. M. Damashek and F.J. Gilman, *Phys. Rev.* D1, 1319 (1970).

25. J.S. Levinger, *Phys. Rev.* 97, 970 (1955).

26. B.M. Chasan, G. Cocconi, V.T. Cocconi, R.M. Schectman and D.H. White, *Phys. Rev.* 119, 811 (1960).

27. C.E. Roos and V.Z. Peterson, *Phys. Rev.* 124, 1610 (1961).

28. F.H. Heimlich, G. Huber, E. RÜssler, P. David, H. Mommsen and D. Wegener, *Nucl. Phys.* A267, 493 (1976).

29. G. Andersson, I. Blomqvist, B. Forkman, G.G. Jonsson, A. Jährund, I. Kroon, K. Lindgren, B. Schrøder and K. Tesch , *Nucl. Phys.* A197, 44 (1972).

30. T.A. Gabriel and R.G. Alsmiller, Jr., *Phys. Rev.* 182, 1035 (1969).

31. K.G. Dedrick, *Revs. Mod. Phys.* 34, 429 (1962).

32. P.A. Benioff, *Phys. Rev.* 119, 324 (1960).

Table 1. Experimental data for (γ,p) reaction (for details see references quoted)

Target Nucleus	Product Nucleus§	Energy Range† (GeV)	Lower and Upper Limits of $\bar{\sigma}_k$ (μb)	Ref.
^{11}B	$^{10}Be^*$	0.15 – 0.80	170 – 330	16
^{16}O	$^{15}N^*$	0.10 – 0.80	Not well defined	15
^{18}O	$^{17}N^*$	0.14 – 0.38	420 – 470 (300 – 330)≠	14
^{30}Si	^{29}Al	0.15 – 0.60	980 –1190	8
^{30}Si	^{29}Al	0.15 – 0.80	990 –1100	19
^{40}Ca	$^{39}K^*$	0.10 – 0.80	Not well defined	18
^{68}Zn	^{67}Cu	0.15 – 0.80	960 –1050	19
^{118}Sn	$^{117}In^{g+m}$	0.15 – 0.80	900 –1000#	17,20
^{130}Te	^{129}Sb	0.15 – 0.80	500 – 600	19

§ The symbol * indicates an excited state of the product nucleus.

† The energy range here indicated refers to that used in the present analysis even if the lower energy limits of the measurements are below 0.15 GeV.

≠ Also indicated are the values obtained after normalization (see text), which have been used in the analysis.

Sum of the yields of the high- and low-spin states.

Table 2. The (γ,n) reaction probabilities, $\phi(k,A)$, as obtained by the present Monte Carlo calculation (true direct process, Appr. III)†

Photon Energy k(GeV)	Target Nucleus														
	^{11}B	^{12}C	^{16}O	^{18}O	^{27}Al	^{30}Si	^{55}Mn	^{68}Zn	^{75}As	^{118}Sn	^{127}I	^{130}Te	^{197}Au	^{209}Bi	^{238}U
0.20	0.096	0.072	0.055	0.065	0.030	0.026	0.000	0.000	0.000	0.000	0.000	0.000	0.000	0.000	0.000
0.22	0.124	0.101	0.087	0.098	0.070	0.065	0.042	0.035	0.033	0.026	0.017	0.019	0.004	0.004	0.003
0.25	0.151	0.130	0.112	0.128	0.096	0.094	0.072	0.066	0.066	0.055	0.050	0.052	0.042	0.039	0.038
0.28	0.149	0.134	0.115	0.126	0.097	0.094	0.078	0.072	0.068	0.058	0.053	0.054	0.044	0.046	0.041
0.30	0.140	0.122	0.110	0.119	0.095	0.089	0.076	0.062	0.067	0.056	0.052	0.052	0.046	0.044	0.044
0.31	0.144	0.121	0.109	0.113	0.090	0.084	0.072	0.063	0.061	0.048	0.052	0.053	0.045	0.046	0.042
0.32	0.130	0.108	0.102	0.100	0.076	0.076	0.056	0.058	0.053	0.041	0.043	0.042	0.037	0.037	0.041
0.35	0.120	0.106	0.092	0.095	0.072	0.065	0.053	0.052	0.048	0.039	0.041	0.040	0.035	0.033	0.031
0.40	0.118	0.107	0.087	0.093	0.072	0.066	0.051	0.043	0.044	0.037	0.036	0.034	0.033	0.029	0.027
0.45	0.126	0.106	0.095	0.098	0.074	0.071	0.050	0.049	0.043	0.035	0.036	0.033	0.030	0.029	0.030
0.50	0.114	0.098	0.079	0.082	0.064	0.045	0.044	0.041	0.039	0.033	0.031	0.033	0.028	0.027	0.025
0.55	0.097	0.086	0.074	0.083	0.061	0.062	0.048	0.044	0.043	0.033	0.036	0.036	0.028	0.028	0.026
0.60	0.103	0.092	0.077	0.085	0.068	0.066	0.053	0.051	0.047	0.038	0.041	0.041	0.032	0.032	0.031
0.70	0.110	0.097	0.092	0.097	0.081	0.079	0.065	0.061	0.060	0.050	0.046	0.048	0.045	0.041	0.042
0.80	0.090	0.078	0.074	0.078	0.050	0.062	0.052	0.052	0.050	0.039	0.041	0.042	0.035	0.036	0.034
0.90	0.088	0.078	0.071	0.075	0.062	0.060	0.053	0.048	0.047	0.040	0.040	0.040	0.036	0.034	0.034
1.00	0.101	0.090	0.082	0.088	0.070	0.069	0.059	0.057	0.055	0.046	0.046	0.049	0.040	0.042	0.038

† Errors (statistical only) associated with the probability values quoted in this Table range from a maximum of ≈ 30% (^{238}U at k = 220 MeV) to a minimum of ≈ 6% (^{11}B at 280 MeV).

Table 3. The (γ,p) reaction probabilities, $\phi(k,A)$, as obtained by the present Monte Carlo calculation (true direct process, Appr. III)†

Photon Energy k(GeV)	Targets Nucleus $^{11}_{5}B$	$^{12}_{6}C$	$^{16}_{8}O$	$^{18}_{8}O$	$^{27}_{13}Al$	$^{30}_{14}Si$	$^{55}_{25}Mn$	$^{68}_{30}Zn$	$^{75}_{33}As$	$^{118}_{50}Sn$	$^{127}_{53}I$	$^{130}_{52}Te$	$^{197}_{79}Au$	$^{209}_{83}Bi$	$^{238}_{92}U$
0.20	0.054	0.054	0.043	0.032	0.022	0.017	0.000	0.000	0.000	0.000	0.000	0.000	0.000	0.000	0.000
0.22	0.085	0.089	0.073	0.057	0.051	0.045	0.025	0.021	0.018	0.011	0.010	0.008	0.005	0.005	0.006
0.25	0.102	0.108	0.094	0.078	0.079	0.071	0.049	0.039	0.038	0.027	0.023	0.025	0.020	0.018	0.016
0.28	0.115	0.114	0.103	0.081	0.071	0.069	0.046	0.039	0.042	0.033	0.031	0.029	0.023	0.023	0.021
0.30	0.111	0.110	0.101	0.081	0.077	0.068	0.051	0.043	0.042	0.032	0.030	0.028	0.021	0.021	0.017
0.31	0.107	0.114	0.095	0.086	0.070	0.065	0.044	0.042	0.041	0.032	0.031	0.031	0.025	0.023	0.018
0.32	0.106	0.111	0.097	0.078	0.063	0.061	0.045	0.039	0.037	0.027	0.027	0.024	0.023	0.019	0.017
0.35	0.098	0.105	0.087	0.071	0.061	0.059	0.038	0.036	0.032	0.026	0.025	0.023	0.020	0.018	0.015
0.40	0.108	0.115	0.103	0.080	0.071	0.065	0.049	0.040	0.039	0.034	0.028	0.029	0.024	0.022	0.021
0.45	0.109	0.112	0.096	0.084	0.073	0.067	0.044	0.041	0.038	0.029	0.026	0.027	0.021	0.023	0.018
0.50	0.092	0.094	0.086	0.068	0.065	0.056	0.042	0.036	0.033	0.027	0.026	0.023	0.019	0.018	0.018
0.55	0.089	0.094	0.083	0.070	0.062	0.057	0.042	0.039	0.036	0.026	0.027	0.026	0.023	0.019	0.019
0.60	0.089	0.091	0.078	0.069	0.063	0.057	0.044	0.041	0.038	0.033	0.028	0.028	0.024	0.022	0.020
0.70	0.088	0.097	0.087	0.072	0.068	0.063	0.047	0.041	0.041	0.035	0.032	0.030	0.027	0.028	0.023
0.80	0.067	0.075	0.068	0.056	0.050	0.052	0.039	0.035	0.034	0.029	0.026	0.026	0.022	0.020	0.021
0.90	0.066	0.069	0.064	0.057	0.053	0.047	0.037	0.033	0.030	0.028	0.026	0.024	0.018	0.021	0.020
1.00	0.081	0.086	0.082	0.067	0.063	0.057	0.047	0.039	0.040	0.031	0.031	0.028	0.026	0.023	0.021

†Errors (statistical only) associated with the probability values quoted in this Table range from a maximum of ≃ 30% (^{238}U at k = 220 MeV) to a minimum of ≃ 7% (^{11}B at 280 MeV).

Table 4. Values of the ratio Q as a function of A

A	N	Z	Q
12	6	6	1.0(76) ± 0.1
27	14	13	1.0(81) ± 0.1
75	42	33	1.0(76) ± 0.1
127	74	53	1.0(66) ± 0.1
209	126	83	1.0(51) ± 0.1
238	146	92	1.0(45) ± 0.1

Table 5. Number of events per 10^4 cascades for (γ,np), (γ,n) and (γ,p) reactions at 0.3 GeV in ^{27}Al.

Type of Primary Interaction	Reaction	State of the Residual Nucleus	Number of Events for $E^* \leq 2$ MeV (N_1)	Number of Events for $E^* \leq 10$ MeV (N_2)	N_1/N_2
Photomesonic	$(\gamma,n)^\dagger$	Cold	963	1013	0.95
Photomesonic	$(\gamma,p)^\dagger$	Cold	827	854	0.97
Quasi-deuteron	(γ,np)	Cold	1151	1151	1.00
Quasi-deuteron	(γ,np)	Hot	150	150	1.00
Photomesonic	(γ,np)	Cold	45	161	0.28
Photomesonic	(γ,np)	Hot	560	444	1.26
Photomesonic plus Quasi-deuteron	(γ,np)	Cold	1196	1312	0.91
Photomesonic plus Quasi-deuteron	(γ,np)	Hot	710	594	1.20

†True direct plus cascade.

FIGURE CAPTIONS

Fig. 1. Plot of available experimental data for (γ,p) mean cross sections per photon above the π-meson photoproduction threshold vs the atomic number Z of the target nucleus. Elongated areas show ranges of uncertainties relative to the measured yields, as explained in the text. Only the following target nuclei have been considered: $^{11}_{5}B$, $^{18}_{8}O$, $^{30}_{14}Si$ (cross), $^{68}_{30}Zn$, $^{118}_{50}Sn$, and $^{130}_{52}Te$ (for experimental details, references, and other related topics, see Table 1) The full straight line represents the result of a least--squares treatment of experimental data (the l.-s. analysis rejected the point relative to ^{30}Si) and gives $\overline{\sigma}_{k(\gamma,p)exp.} = (115\pm15)Z^{(0.50\pm0.05)}$ μb. The dashed line results from a least-squares fite of data obtained by the Monte Carlo calculation for *true direct* (γ,p) reactions and will be discussed in the text. Both straight lines have been back-extrapolated down to Z = 1 for reasons which will be clear forth.

Fig. 2. Plot of the Monte Carlo mean cross section values of (γ,n) reaction vs mass number A of the target nucleus. Open circles: Appr. I; crosses; Appr. II; filled circles: Appr. III (see text for further details). The full straight line represents the result of a least-squares treatment of the calculated values for Appr. III and the shadowed region shows the range of statistical uncertainty as obtained from the fit (three points relative to ^{7}Li, ^{9}Be, and ^{11}B were rejected). The trends given in [10] (*dashed line with* shadowed area) and arising from an A^{1}--dependence (dashed line) are also shown for comparison.

Fig. 3. The same as Fig. 2 for (γ,p) reaction. The data rejected in the least-squares analysis are those relative to ^{12}C and ^{16}O. No comparison with experiment is shown, for it has already been made in Fig. 1.

Fig. 4. The figure shows the trend of the ratio R (expressed as per cent) of the sum of *cold* (γ,π^+), (γ,π^-), and (γ,π^0) events to the total (*hot* plus *cold*) events of the same type vs the incident photon energy, k. Five excitation energies E^*, from 2 MeV to 40 MeV, were considered. The curves were calculated for the ^{27}Al target. Quite similar trends, however, were found from other nuclei.

Fig. 5. Calculated points and least-squares trend (full line) of *true direct* (γ,n) mean cross section per photon vs neutron number N of the target nucleus. The points were calculated following Appr. III. For comparison, the trends relative to a *surface production model* and a *volume production model* (without any hindrance factor) have been shown and marked $N^{2/3}$ and N^1, respectively.

Fig. 6. The same as Fig. 5, for (γ,p) true direct reaction (Appr. III). The first two points were rejected in the fitting procedure used to obtain the trend represented as a full line (see also Fig. 1 for comparison with experimental data).

Fig. 7. Cross sections of the (γ,n) reaction in ^{12}C. For details see text.

Fig. 8. The same as Fig. 7. (γ,p) reaction in ^{30}Si.

Fig. 9. The same as Fig. 7. (γ,p) reaction in ^{68}Zn.

Fig. 10. The same as Fig. 7. (γ,p) reaction in ^{118}Sn.

Fig. 11. The same as Fig. 7. (γ,p) reaction in ^{130}Te.

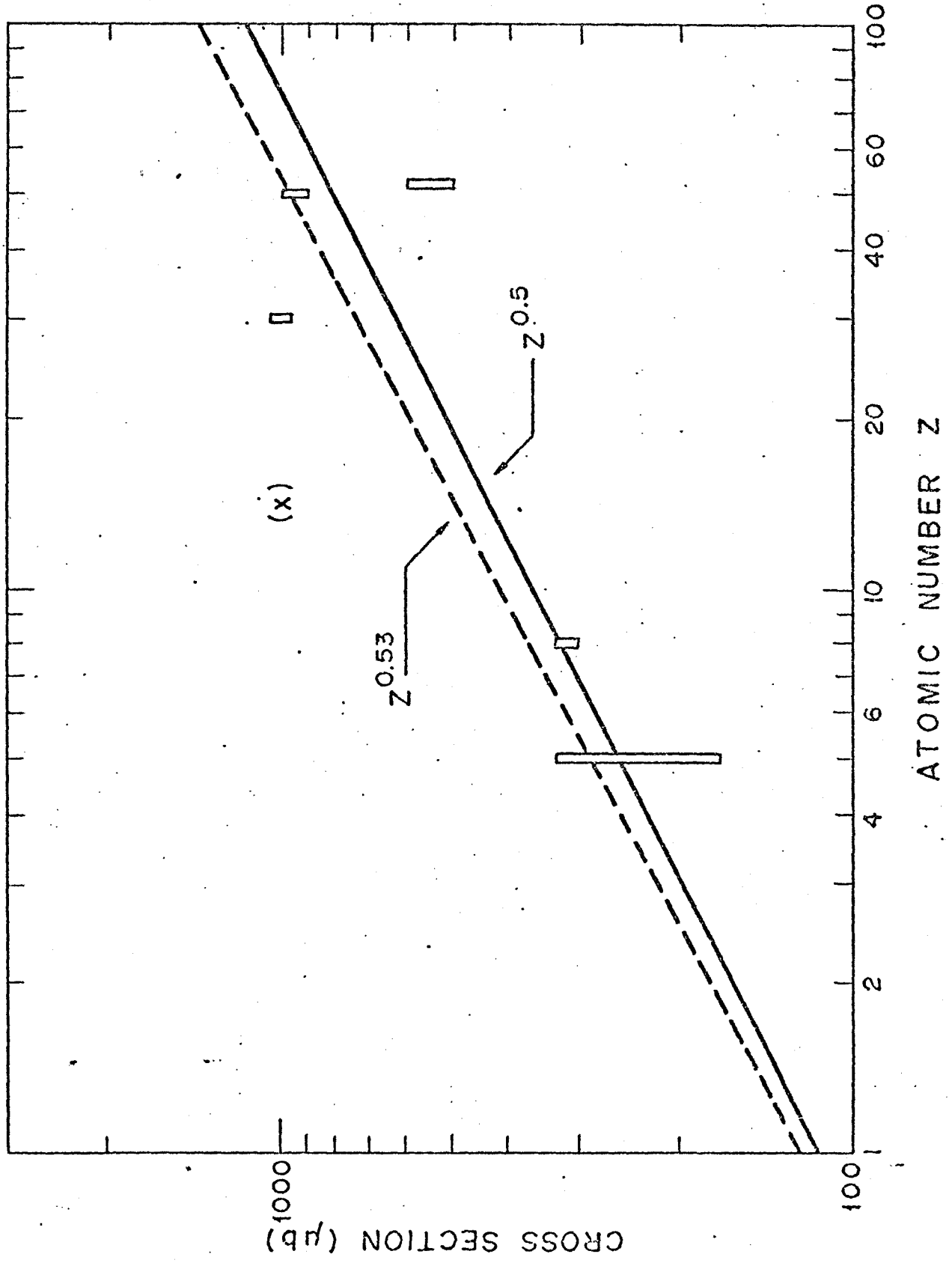
CROSS SECTION (μb)
1000
100
1
2
4
6
10
20
40
60
100
ATOMIC NUMBER Z
(x)
$Z^{0.5}$
$Z^{0.53}$

Figura 1

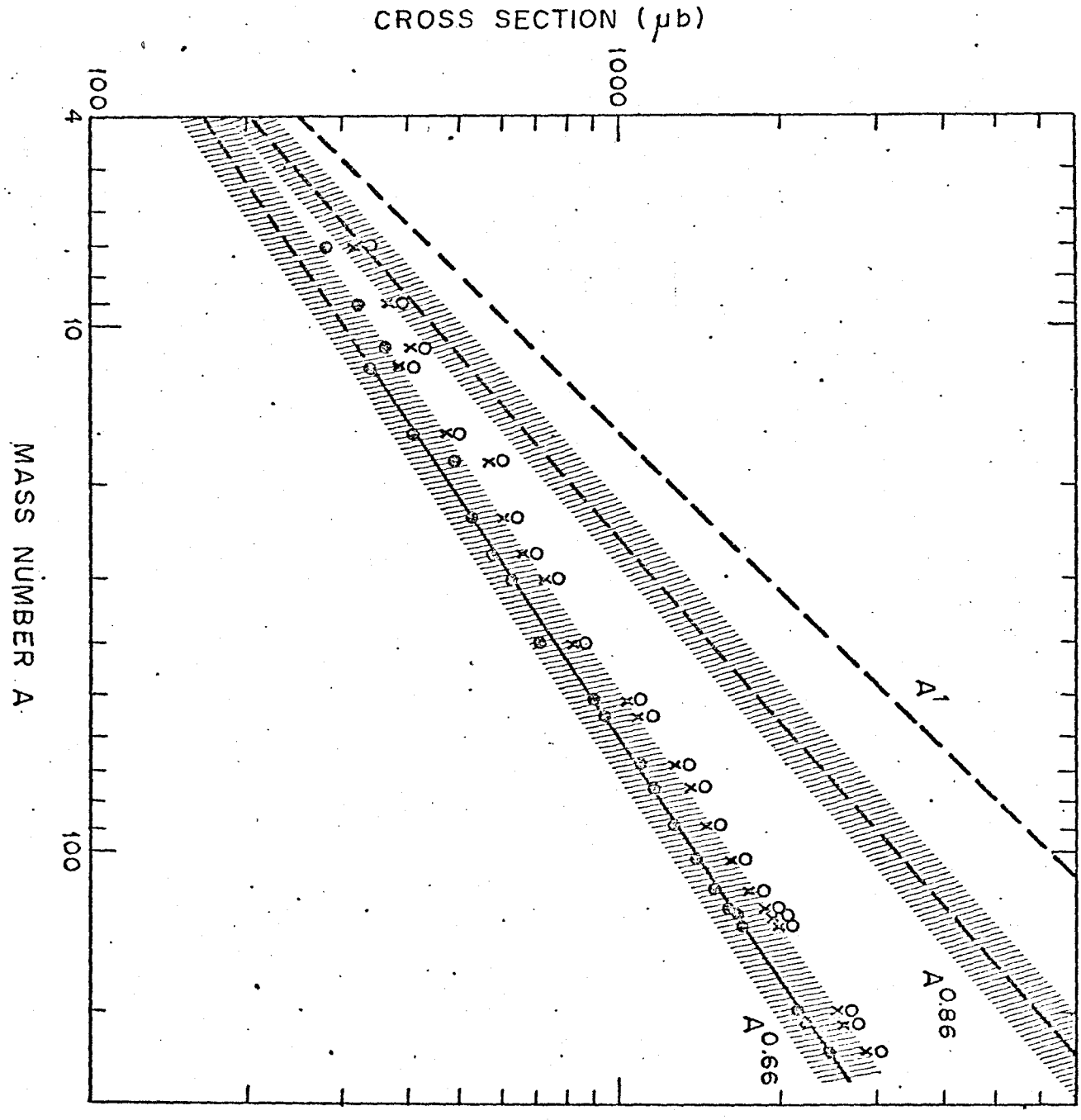

Figura 2

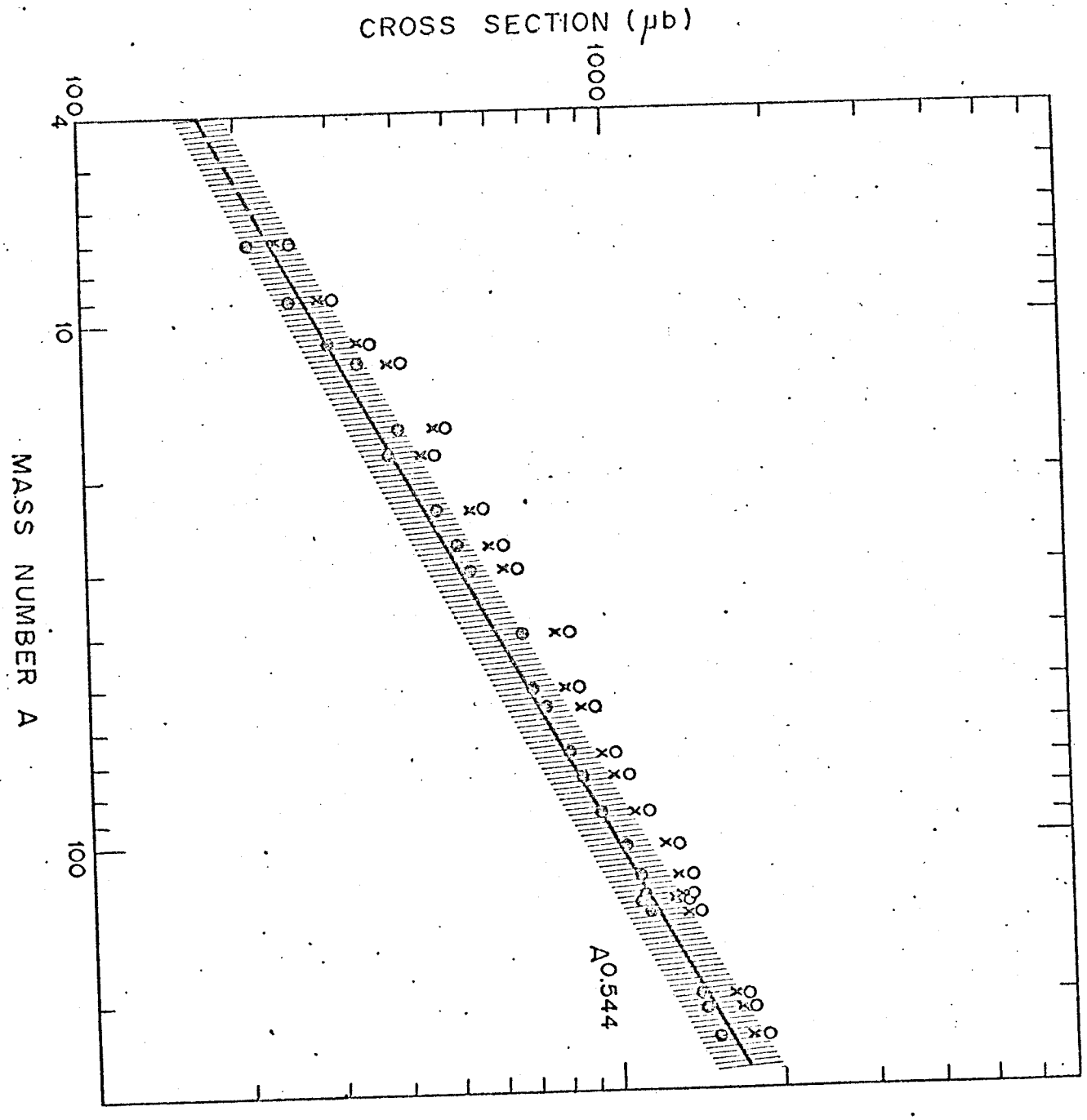

Figura 3

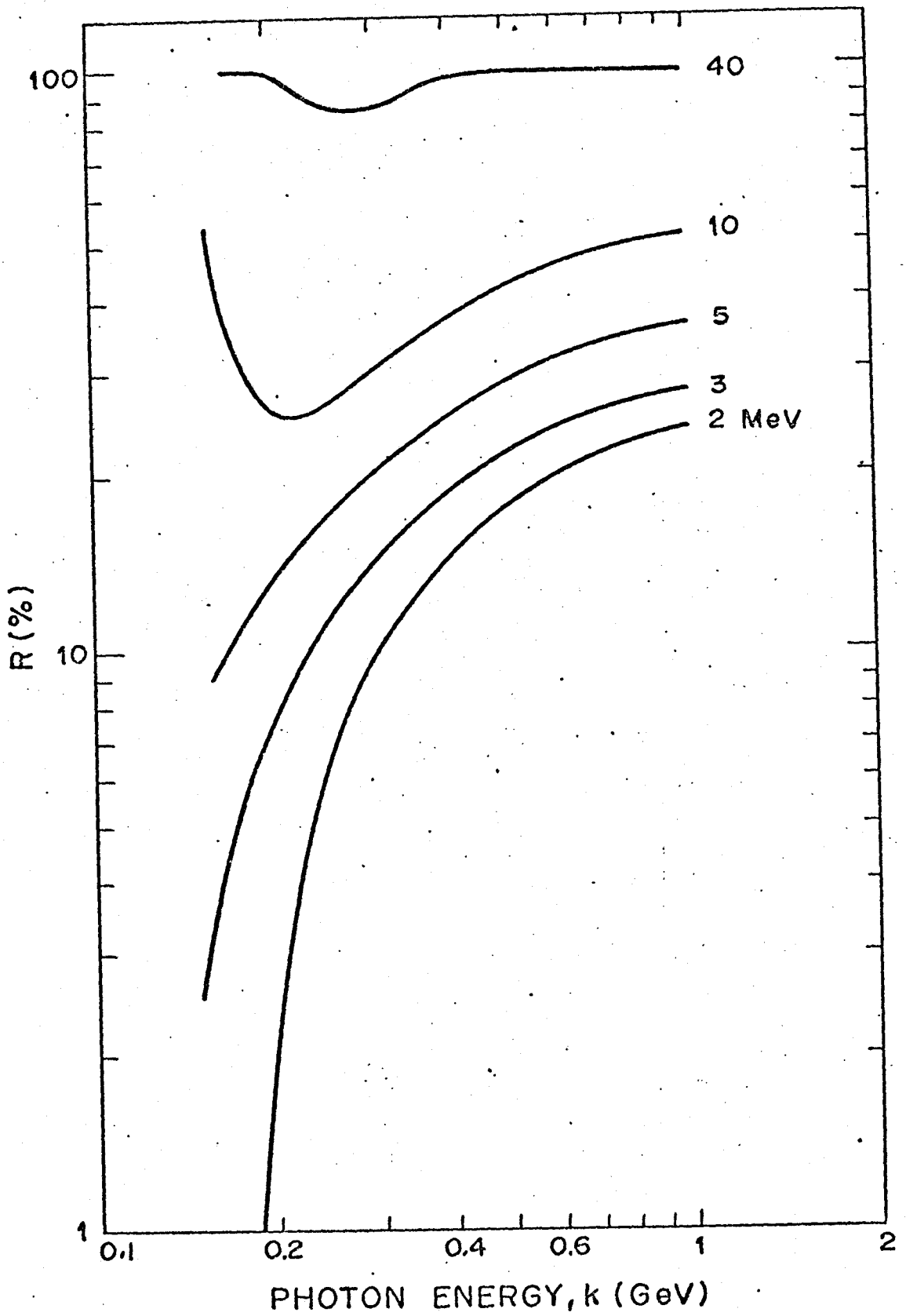

Figura 4

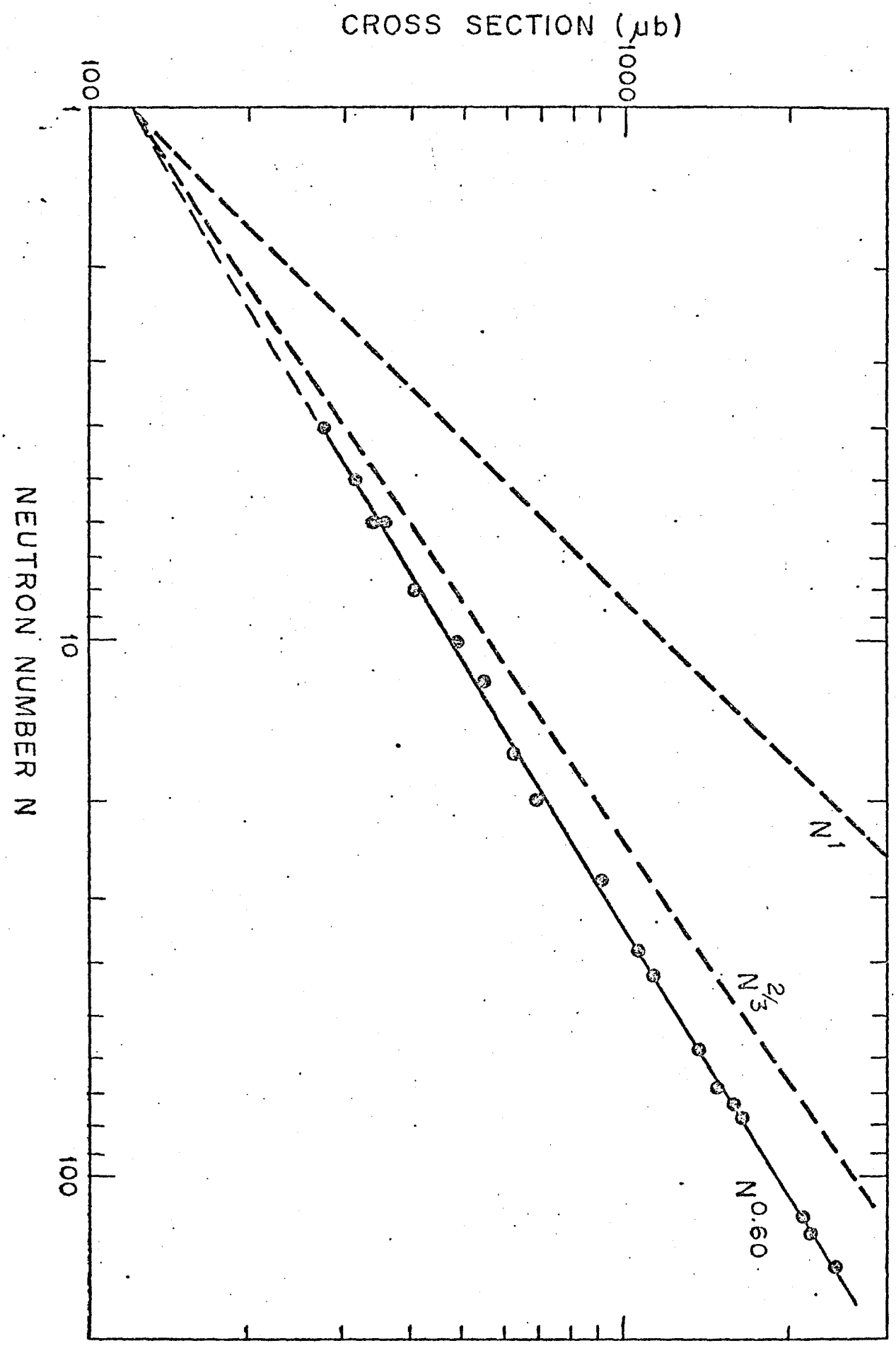
CROSS SECTION (μb)
100
1000
1
10
100
NEUTRON NUMBER N
N1
N3/2
N0.60

Figura 5

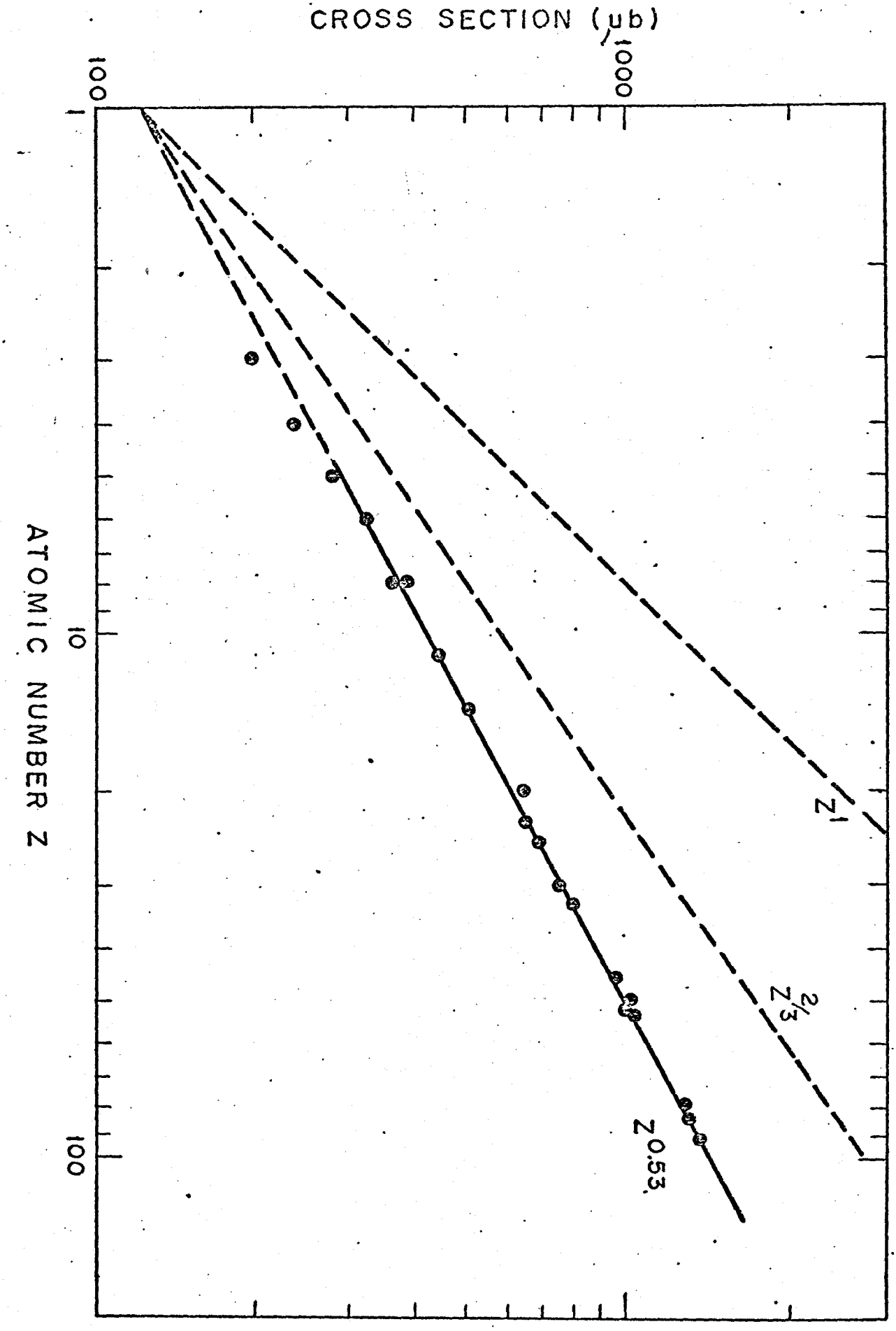

Figura 6.

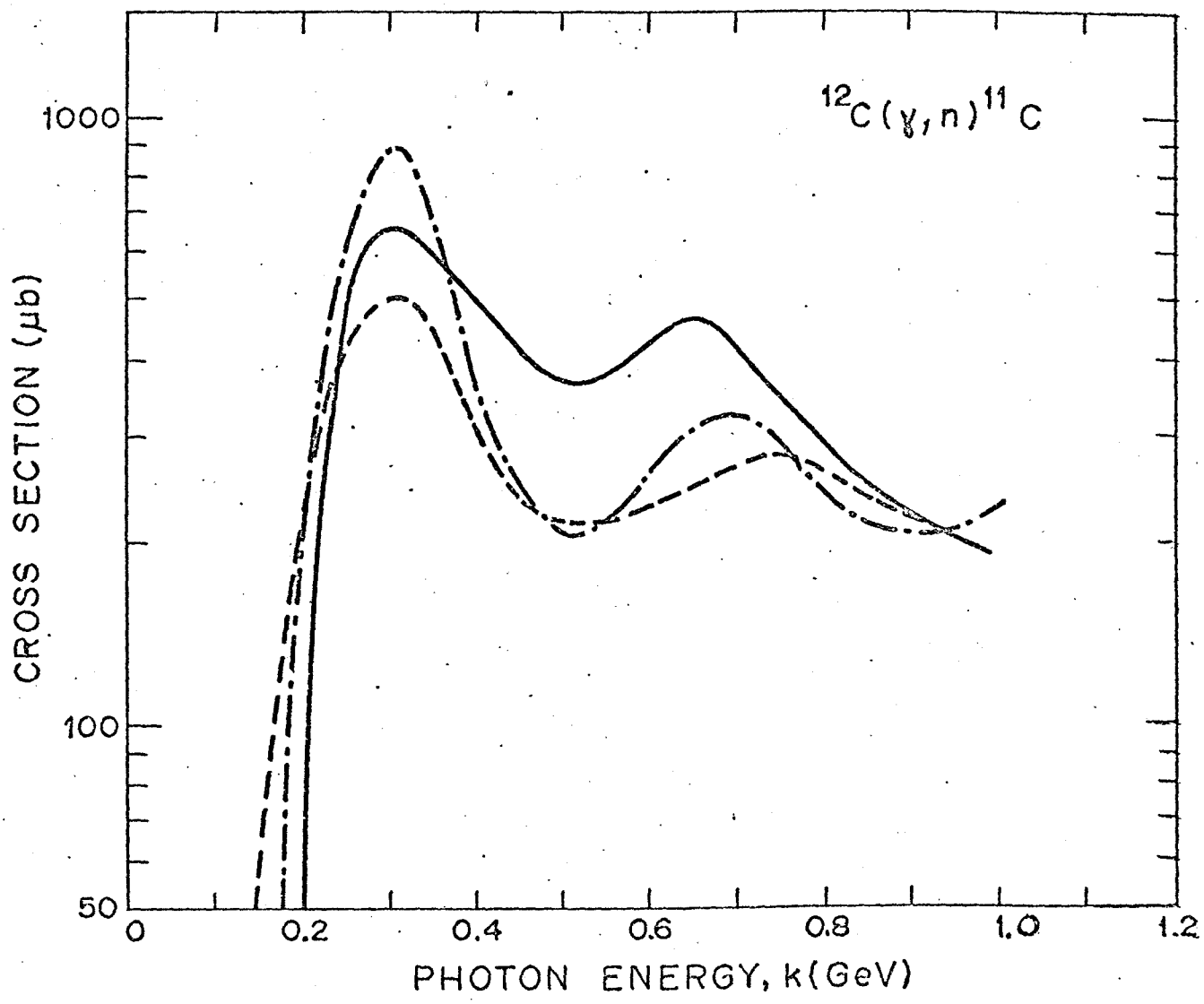
$^{12}C(\gamma,n)^{11}C$
1000
100
50
CROSS SECTION (μb)
0
0.2
0.4
0.6
0.8
1.0
1.2
PHOTON ENERGY, k(GeV)

Figura 7

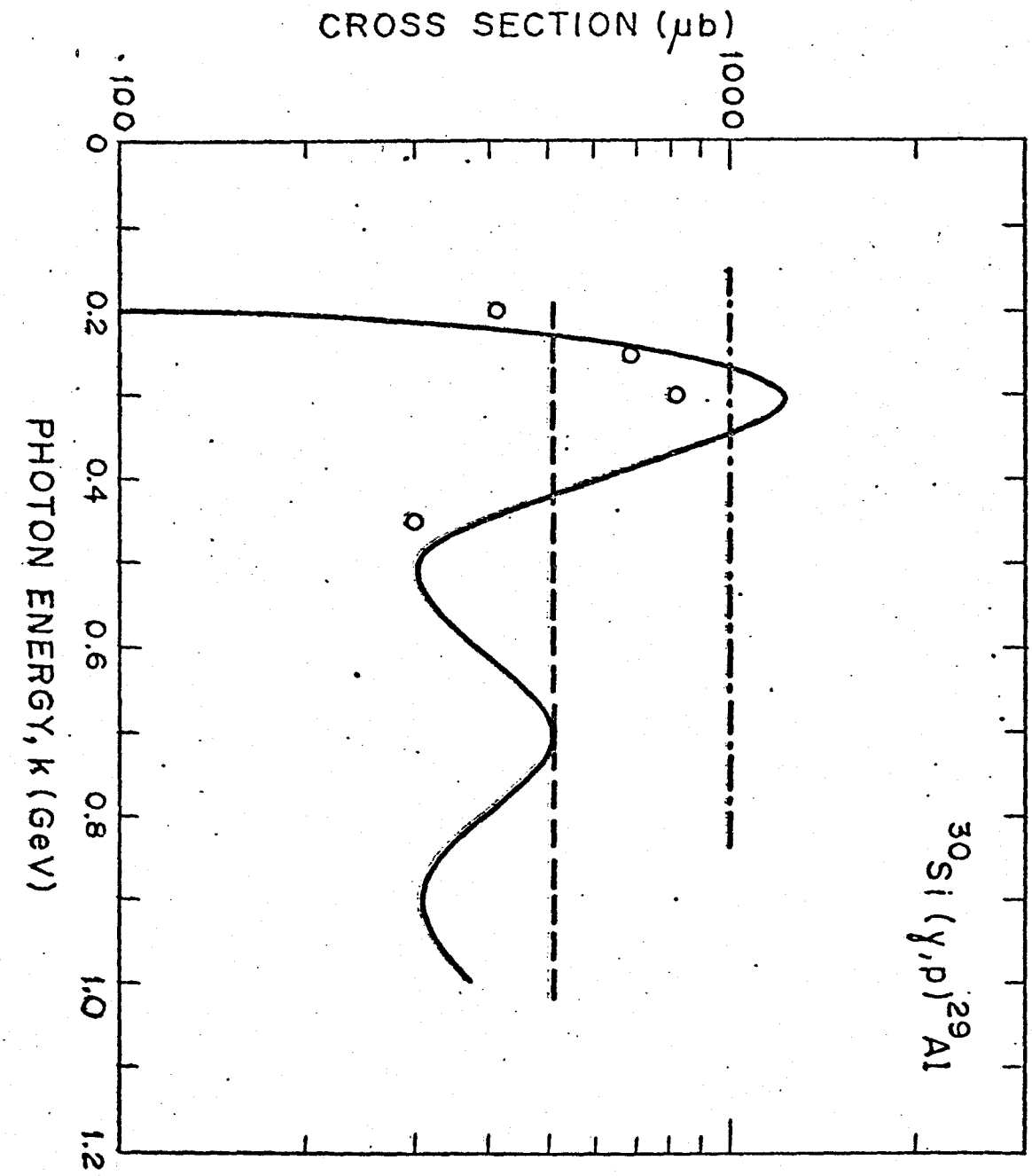
CROSS SECTION (μb)
100
1000
0
0.2
0.4
0.6
0.8
1.0
1.2
PHOTON ENERGY, K (GeV)
$^{30}Si(\gamma,p)^{29}Al$

Figura 8

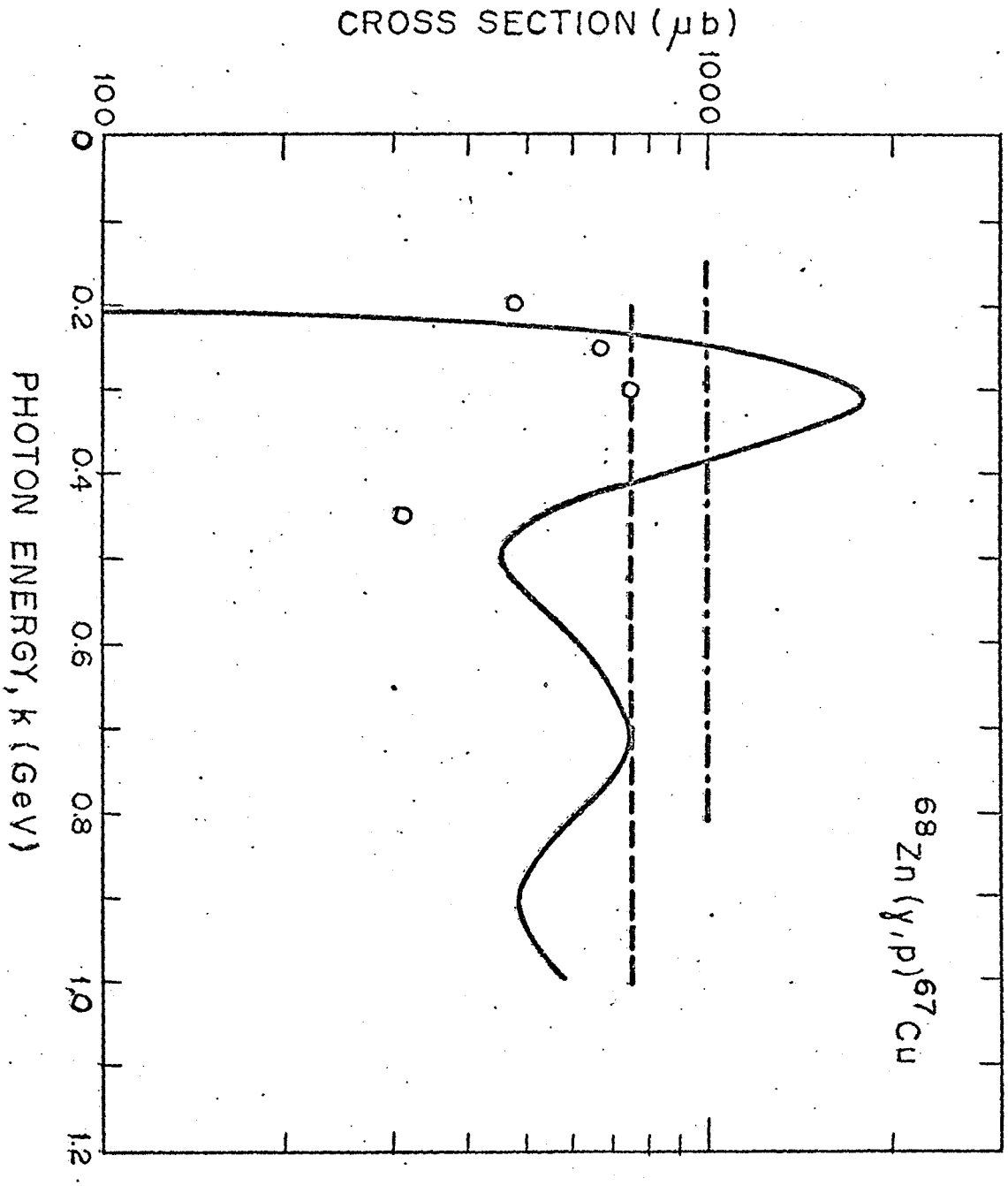
CROSS SECTION (μb)
100
1000
0
0.2
0.4
0.6
0.8
1.0
1.2
PHOTON ENERGY, k (GeV)
$^{68}Zn(\gamma,p)^{67}Cu$

Figura 9

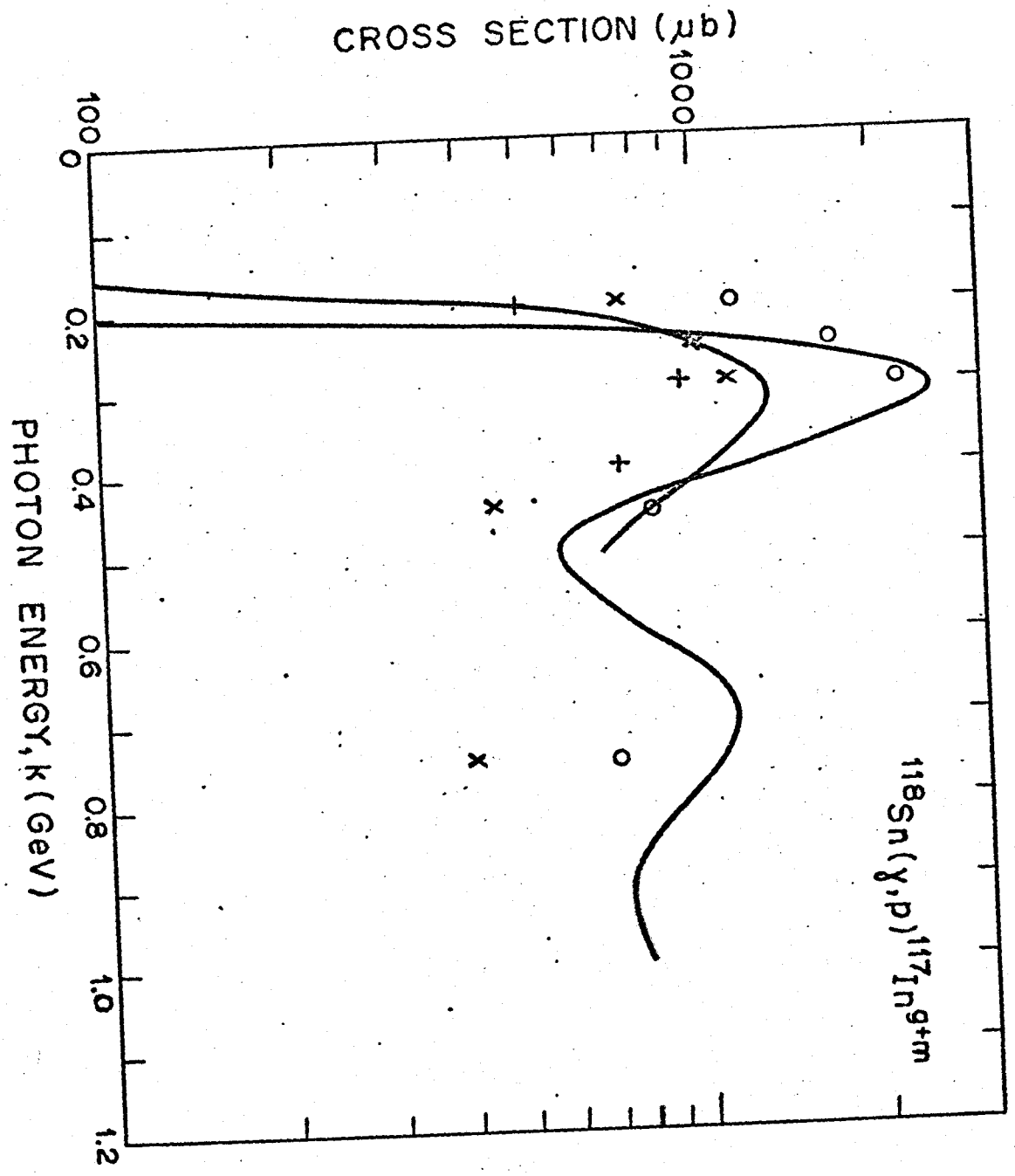
CROSS SECTION (μb)
1000
100
0
0.2
0.4
0.6
0.8
1.0
1.2
PHOTON ENERGY, k (GeV)
$^{118}Sn(\gamma,p)^{117}In^{g+m}$

Figura 10

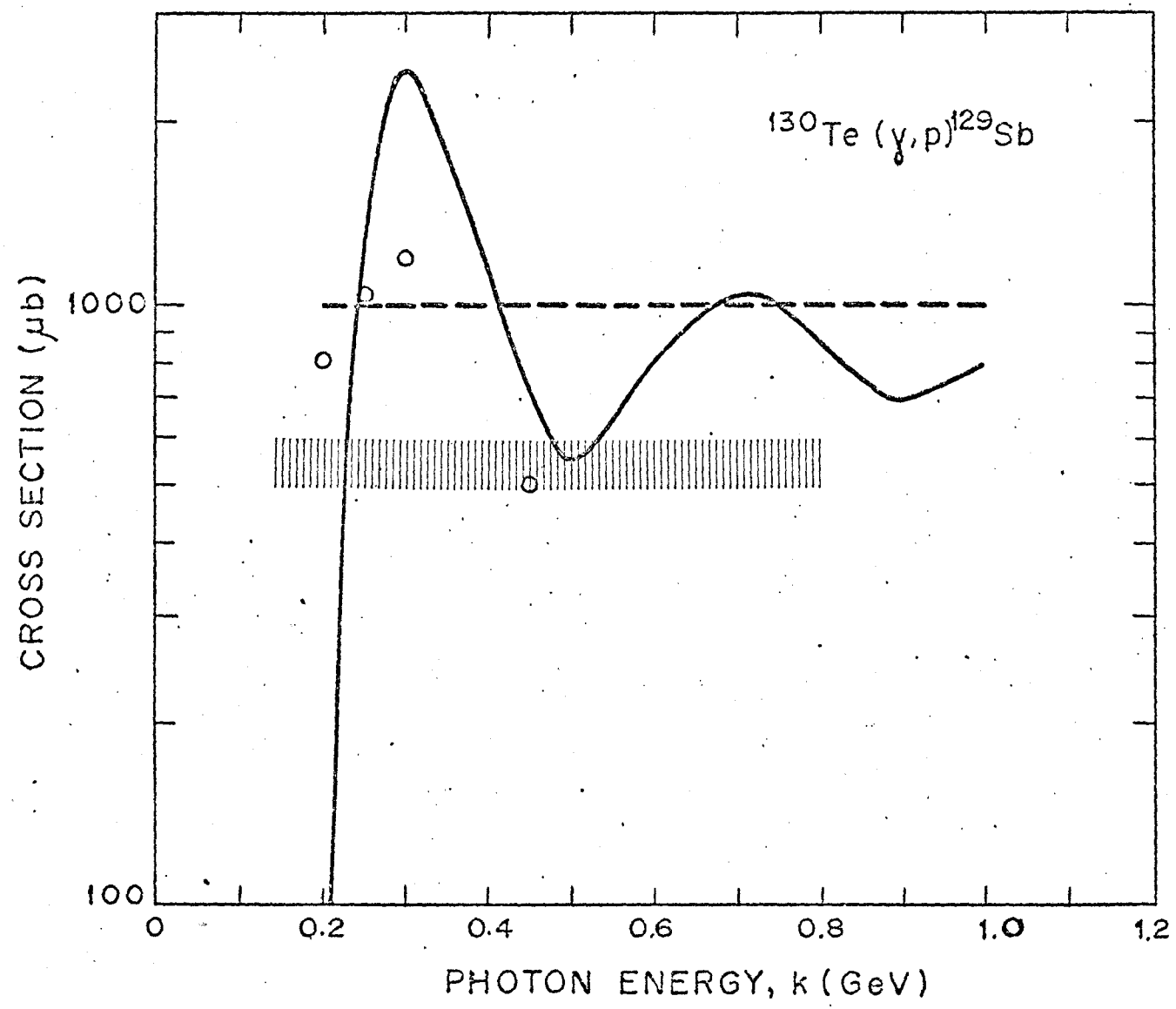
$^{130}Te\ (\gamma,p)^{129}Sb$
CROSS SECTION (μb)
1000
100
0
0.2
0.4
0.6
0.8
1.0
1.2
PHOTON ENERGY, k (GeV)

Figura 11

O CBPF PUBLICA PERIODICAMENTE AS DUAS SÉRIES DE RELATÓRIO A SEGUIR.

SÉRIE A: PRÉ — PUBLICAÇÃO DE RELATÓRIOS DE TRABALHOS QUE NECESSITAM DE RÁPIDA CIRCULAÇÃO.

SÉRIE B TRABALHOS ORIGINAIS, MONOGRAFIAS, TABELAS E OUTROS DADOS NÃO DESTINADOS A PUBLICAÇÃO.

CBPF PUBLISHES PERIODICALLY THE FOLLOWING TWO SERIES OF REPORTS:

SERIES A: PRE - PUBLICATION OF REPORTS OF PAPERS NEEDING QUICK CIRCULATION.

SERIES B: ORIGINAL PAPERS, MONOGRAPHIES, TABLES AND OTHER DATA WHICH ARE NOT INTENDED TO BE PUBLISHED ELSEWHERE.

PEDIDOS DE CÓPIA DESTE RELATÓRIO FAVOR DIRIGIR-SE A:

REQUEST FOR COPY OF THIS REPORT PLEASE ADDRESS TO:

BIBLIOTECÁRIA - CHEFE
CBPF
AV. WENCESLAU BRAZ, 71 FUNDOS, ZC-82
RIO DE JANEIRO, RJ 20.000
BRASIL